Journal Pre-proof

Self-assembly of activated lipase hybrid nanoflowers with superior activity and enhanced stability

Conghai Li, Juan Zhao, Zhijin Zhang, Yanjun Jiang, Muhammad Bilal, Yunhong Jiang, Shiru Jia, Jiandong Cui

PII: S1369-703X(20)30097-8

DOI: https://doi.org/10.1016/j.bej.2020.107582

Reference: BEJ 107582

To appear in: *Biochemical Engineering Journal*

Received Date: 7 December 2019

Revised Date: 2 March 2020

Accepted Date: 1 April 2020

Please cite this article as: Li C, Zhao J, Zhang Z, Jiang Y, Bilal M, Jiang Y, Jia S, Cui J, Self-assembly of activated lipase hybrid nanoflowers with superior activity and enhanced stability, *Biochemical Engineering Journal* (2020), doi: https://doi.org/10.1016/j.bej.2020.107582

Self-assembly of activated lipase hybrid nanoflowers with superior activity and enhanced stability

Conghai Li[1], Juan Zhao[2], Zhijin Zhang[1], Yanjun Jiang[3], Muhammad Bilal[4], Yunhong Jiang[5], Shiru Jia[1] Jiandong Cui[1*]

[1]State Key Laboratory of Food Nutrition and Safety, Tianjin University of Science and Technology, Tianjin 300457, China; Key Laboratory of Industrial Fermentation Microbiology, Ministry of Education, Tianjin University of Science and Technology, Tianjin 300457, China

[2]Research Centre of Modern Analysis Technology, Tianjin University of Science and Technology, Tianjin 300457, China

[3]School of Chemical Engineering and Technology, Hebei University of Technology, 8 Guangrong Road, Hongqiao District, Tianjin, 300130, PR China

[4]School of Life Science and Food Engineering, Huaiyin Institute of Technology, Huaian 223003, PR China.

[5]HBBE, Department of Applied Science, Northumbria University, Newcastle, NE1 8ST, United Kingdom.

[*] Corresponding authors:

Jiandong Cui, E-mail: cjd007cn@163.com, Tel: +86-022-60601598

Highlights

- A new activated hNF-lipase was synthesized
- Ca^{2+} not only induced self-assemble of nanoflowers, but also activated the

lipase from *A. oryzae*.

- Tween-80 acts as an excellent activator for lipase from *A. oryzae*.
- The activated hNF-lipase exerted enhanced enzymatic and stability.

The first two authors contributed equally to this paper

Abstract

Lipase-inorganic hybrid nanoflowers were prepared using $Ca_3(PO_4)_2$ as the inorganic component and lipase from *Aspergillus oryzae* (*A. oryzae*) as the organic component. The influences of metal ions with different valence, various additives (surfactant), and synthesis conditions on the activity of the lipase hybrid nanoflowers were systematically investigated. Results revealed that the valence state of metal ions played an important role on the shape and activity of lipase hybrid nanoflowers. The synthesized lipase hybrid nanoflowers using bivalence metal ions (Ca^{2+}, Mn^{2+}, and Zn^{2+}) as the inorganic components exhibited relative high activity. However, very low activities were observed in the lipase hybrid nanoflowers using univalent metal ions (Ag^{+}) or trivalent metal ions (Al^{3+}, Fe^{3+}). More importantly, Ca^{2+} not only induced self-assemble of lipase hybrid nanoflowers, but also activated the enzyme activity by inducing conformational changes in lipase from *A. oryzae*. As a result,

lipase/$Ca_3(PO_4)_2$ hybrid nanoflowers (hNF-lipase) exhibited the high activity. The hNF-lipase displayed 9, 12, and 61 folds higher activity than lipase/Ag_3PO_4 hybrid nanoflowers, lipase/$AlPO_4$ hybrid nanoflowers, and lipase/$FePO_4$ nanoflowers, respectively. Compared with free lipase, the hNF-lipase displayed 172% increase in activities by using 0.15 mM Tween-80 as an activity inducer (activated hNF-lipase). Furthermore, the hNF-lipase and activated hNF-lipase exhibited increased stability against high temperature and denaturant, and had good storage stability and reusability.

Keywords: Hybrid nanoflowers; Enzyme immobilization; Lipase; Biocatalysis

1. Introduction

Enzymes are widely used in food ingredients, pharmaceutical and fine chemical industry due to their excellent biocatalytic efficiency [1-4]. However, free enzymes are extremely expensive, and display low stability in non-natural environments such as at high temperature and in the organic solvents that hinder their industrial applicability [5]. Some methods such as DNA operation and chemical modification were made to address these issues [6-8]. Unfortunately, these methods are complex, expensive, and time-consuming for commercial application [9, 10]. In contrast, immobilization of enzymes on/in materials has been recognized as a promising approach that can overcome these limitations due to convenience in handling, recyclable use, and improvement in stability. In the past twenty years, novel materials such as hydrogels, polymer resins, magnetic nanoparticles, carbon nanotubes, gold nanoparticles, and ordered mesoporous silica have been used as supports to engineer

immobilized enzymes [14-19]. Moreover, various immobilization methods involving adsorption, encapsulation, cross-linking, and covalent binding have been utilized to improve the performances of the enzymes [20-23]. However, most of the immobilized enzymes exhibited lower activities than the free forms due to the change of enzyme conformation, and the enhanced diffusion resistance between substrate and enzymes [11-13]. Recently, Ge et al. have reported an elegant approach in enzyme immobilization [24]. The immobilized enzymes were called "enzymes-inorganic hybrid nanoflowers". Compared with the conventional immobilized enzymes, enzymes-inorganic hybrid nanoflowers exhibited better catalytic performances than free enzymes. Lin et al. synthesized trypsin hybrid nanoflowers using $Cu_3(PO_4)_3$ as the inorganic components. The prepared hybrid nanoflowers showed 270% enhancement in enzymatic activity [25]. Similarly, Yin et al. used calcium chloride as the inorganic components to prepare α-chymotrypsin-inorganic hybrid nanoflowers that exhibited 266% increase in catalytic activity compared with free α-chymotrypsin [26]. Besides, lipase/$Zn_3(PO_4)_3$ hybrid nanoflowers were synthesized by Zhang et al [27]. The prepared lipase nanoflowers exhibited 147% higher activity than free lipase. So far, systematic study on the influencing factors of the enzymatic activity of nanoflower is still lacking. Therefore, further investigation is necessary to explore the factors that affecting its enzyme activity.

Lipase is a widely used biocatalyst in the food, chemical, and pharmaceutical industry, which can catalyze the reactions of ester synthesis, hydrolysis, inter-esterification, and trans-esterification [28-34]. However, free lipase exhibits poor operational stability,

sensitivity to harsh environments and difficulty in recycling. Additionally, majority of the lipases presents partial inactivation or total inactivation in solution due to interface effect [35]. Lipase activity can be dramatically increased by the interfacial activation. In our previous study, a lipase hybrid nanoflower with high activity was prepared by interfacial activation, and displayed 4.60-folds high activity compared with free lipase [28]. Generally, metal ions play an important role in the morphology and activity of hybrid nanoflowers [27,28]. Until now, there have been only few reports specifically on metal ion with different valence [29,30]. In this study, the effects of metal ions with different valence, different additives (surfactant), and synthesis conditions such as phosphate radical concentration, lipase concentration, metal ions concentration, and pH on the activity of the lipase nanoflowers were systematically investigated. The stabilities of the resultant hNF-lipase were evaluated. Furthermore, the changes in the secondary structure of lipase nanoflowers were examined.

2. **Materials and methods**

2.1 Materials

Lipase from *Aspergillus oryzae* and P-Nitrophenol (p-NP) were purchased from Sigma-Aldrich. P-Nitrophenyl palmitate (p-NPP), fluorescein isothiocyanate (FITC), copper sulfate pentahydrate, zinc acetate, silver nitrate, iron chloride hexahydrate, and aluminum chloride hexahydrate were provided by International Aladdin Reagent Inc. (Shanghai, China). Dodecyl trimethyl ammonium bromide (DTAB), Tween-80, hexadecyl trimethyl ammonium bromide (CTAB), and triton X-100 were obtained

from Beijing Solarbio Science and Technology Co., Ltd (Beijing, China).

2.2 Effects of metal ions with different valence on the morphology and activity of hNFs-lipase

hNFs-lipase were synthesized according to a previous report with a minor modification [36]. Phosphate buffered saline (PBS, 4 mM, pH 7.4, 6 mL) containing lipase were mixed with 200 mM of each water solution of metal salt (100 μl, $AgNO_3$, $CaCl_2$, $MgCl_2$, $ZnSO_4$, $MnCl_2$, $FeCl_3$, and $AlCl_3$), and incubated at 4 °C for 24 h. Then the precipitates were collected by centrifugation at 11,000 ×g for 5 min, washed with deionized water for three times and dried by vacuum freeze. The amount of lipase in solution before and after the immobilization was quantified by the Bradford method. The relative activity of hNFs-lipase was calculated using the relation given in Eq. (1):

$$\textbf{Relative activity}\ (\%) = \frac{\textbf{total activity of hNF} - \textbf{lipase}}{\textbf{total activity of free lipase used for hNF} - \textbf{lipase}}$$

(Eq. 1)

*2.3 Effects of synthesis conditions on activity of lipase/$Ca_3(PO_4)_2$ hybrid nanoflowers (*hNF-lipase*)*

The effects of lipase concentration (0.01-0.08 mg/mL), $CaCl_2$ concentration (3.28-23.53 mM. Equivalent to adding 16-118 μL of 200 mM $CaCl_2$ solution), phosphate radical concentration (1-10 mM), and pH value (6-11) were investigated on the activity of the hNF-lipase, and the relative activity was measured.

2.4 Effects of surfactants on the activity of lipase/$Ca_3(PO_4)_2$ hybrid nanoflowers (activated hNF-lipase)

Influence of four different surfactants including CTAB, DTAB, TX-100, and Tween

80 was also examined on the activity of the hNF-lipase. Briefly, lipase solution (24.6 mg/mL, 100000 U/g) and appropriate amounts of surfactant were added into 4 mM PBS (pH 7.4), and stirred at 4 °C for 1 h. Subsequently, appropriate amounts of $CaCl_2$ solution (200 mM) was added into the mixtures, and allowed to incubate at 4 °C for 12 hours. Finally, the precipitates were recovered by centrifugation, and washed with deionized water for three times.

2.5 Labeled lipase with fluorescein isothiocyanate

Firstly, 50 mg/mL of FITC solution (FITC in 8 mL dimethyl sulfoxide) was added into 200nM PBS (PH 8.0) containing 1 g lipase for 10 min. After that, the labeled lipase with FITC was immobilized as hNFs-lipase.

2.6 Activity assay

The activities of free lipase, hNF-lipase, and activated hNF-lipase were determined by hydrolysis of p-NPP to p-NP based on the method of Gao with some modifications [37]. Briefly, 0.2 mL p-NPP solution was mixed with 2.8 mL PBS-(TX-100) in colorimetric tube. After ultrasonic emulsification, the mixture solution was incubated for 5 min at 37 °C. Subsequently, lipase samples were added into the above solution to start hydrolysis reaction. After reaction 4.5 min, the mixture was centrifuged and the supernatant were measured at 410 nm using a UV spectrophotometer. One unit of lipase activity was defined as the amount of enzyme liberating 1 μmol of pNP from pNPP per minute.

2.7 Effects of temperature and pH on the activity of the hybrid nanoflowers

The optimum temperatures of lipase samples were measured by incorporating lipase

samples to substrate solution at various temperatures (ranged from 20-60 °C) for 20 min. The relative activity was measured following the activity assay as described above. The optimal pH of lipase samples was determined by incubating them at varying pH ranging from 6.5-8.5.

2.8 Kinetic constant

K_m and V_{max} of lipase samples were determined by using the Michaelis-Menten model. The enzymatic reaction was carried out in the substrate concentration range of 0.05-0.3 mM at a constant enzyme concentration. K_m and V_{max} values were obtained from the Lineweaver-Burk double-reciprocal plot.

2.9 Characterization methods

Scanning electron microscope (SEM, SU-1510, HITACHI, Japan) was used to observe the shapes of hNF-lipase. Fourier transform infrared (FTIR) spectra were obtained on an apparatus (Nicolet iS50, Thermo Fisher Scientific, USA) in the range of 400-4000 cm^{-1}. The secondary structure element content was determined according to the method described by Yang et al [38]. An power x-ray diffraction (D/Max-2500 diffractometer, Shimadzu, Japan) was used to measure the crystal structures of the hNF-lipase at 40 kV and 40 mA. The labeled lipase with FITC hybrid nanoflowers was characterized by confocal laser scanning microscopy (CLSM) (FV1000, Olympus Japan). An energy-dispersive spectrometer (EDS) (Apreo, FEI, USA) was used to determine the elemental composition of the hNF-lipase.

2.10 The stability of lipase samples

The thermal stability of lipase samples was measured by incubating them in PBS (10

mM) at 55 °C for 30 min, and the residual activity was tested. The stability of lipase samples against denaturants was evaluated by testing their residual activities after incubation in different denaturants (95% ethanol, 6 M urea, and 2% SDS) for 30 min. The storage stability of lipase samples was tested at 25 °C for 27 days, and their residual activities were assayed every 3 days. The reusability of immobilized lipase was determined by repeated hydrolysis of NPP, After the completion of one cycle, the immobilized lipase was separated by membrane filtration and washed them with deionized water for three times, and then carried out the next cycle. The residual activity of each cycle was determined.

3. Results and discussion

3.1 Preparation and characterization of the hNF-lipase

The schematic diagram for the synthesis of the hNF-lipase and activated hNF-lipase was presented in Fig. 1. The morphology analysis of the hNF-lipase by SEM clearly revealed that the nanoflower exhibited flower-like shape (Fig. 2a) and was further confirmed by TEM images (Fig. 2b). The results demonstrated that lipase promoted the anisotropic growth of $Ca_3(PO_4)_2$ crystals and the formation of flower-like structure [39]. The CLSM image showed that immobilization of lipase was immobilized onto the hNF-lipase because fluorescein isothiocyanate (FITC) labeled lipase protein exhibited strong green fluorescence (Fig. 2c). In addition, the presence of C and N were also found in the lipase nanoflowers when conducted the EDS experiment (Fig. 3a). However, no C and N elements were not found in the pure $Ca_3(PO_4)_2$ (Fig. 3b). The results demonstrated that lipase was embedded in the hNF-lipase. FTIR spectral

analysis indicated the appearance of numerous peaks at different wavenumbers (Fig. 4a). The characteristic peaks at 1655 cm^{-1} and 1542 cm^{-1} were derived from stretching vibration of C=O and N-H in amide I and amide II, respectively, which revealed the presence of lipase. Typical peaks at 1027 cm^{-1} were assigned to vibration of PO_4^{3-}, indicating the existence of $Ca_3(PO_4)_2$ in the hNF-lipase. In addition, power x-ray diffraction (PXRD) was conducted in the range of 5-100° to explore the crystal structure of the lipase nanoflowers. The results are shown in Fig. 4b. Both hNF-lipase and activated hNF-lipase had similar the diffraction peaks, representing that surfactants did not influenced the crystalline structure of hNF-lipase. Furthermore, the positions and relative intensities of all diffraction peaks of hNF-lipase and $Ca_3(PO_4)_2$ matched well with those obtained from the JCPDS card (18-0303)(Fig. 4c) [26,42]. These results indicated that lipase/$Ca_3(PO_4)_2$ hybrid nanoflowers were synthesized successfully.

3.2 Influences of metal ions with different valence on the morphology and activity of hNF-lipase

As shown in Fig. 5, the hNF-lipase/$Ca_3(PO_4)_2$ and hNF-lipase/$Mn_3(PO_4)_2$ have a hierarchical like flower morphology (Fig. 5b and 5c). However, the lipase/Ag_3PO_4 hybrid nanoflowers, lipase/$Zn_3(PO_4)_2$ hybrid nanoflowers, lipase/$AlPO_4$ hybrid nanoflowers, and lipase/$FePO_4$ hybrid nanoflowers exhibit large amorphous clusters(Fig. 5a, 5d, 5e, 5f). These results showed that the morphology of the hNF-lipase is depended on the metal used. The previous reports also suggested that lipase hybrid nanoflowers from porcine pancreas exhibited compact spherical shape

when zinc phosphate was used as the inorganic component. However, the lipase hybrid nanoflowers displayed like flower shape when zinc phosphate was used as the inorganic component [39, 40]. In addition, the influences of metal ions with different valence on the activity of hNF-lipase were also investigated. The results were shown in Table 1, low activity was observed for the lipase/$FePO_4$ hybrid nanoflowers, lipase/$AlPO_4$ hybrid nanoflowers, and lipase/Ag_3PO_4 hybrid nanoflowers. No nanoflower precipitates were observed when magnesium phosphate was used as the inorganic component. In contrast, the lipase/$Mn_3(PO_4)_2$ hybrid nanoflowers, lipase/$Zn_3(PO_4)_2$ hybrid nanoflowers, and lipase/$Ca_3(PO_4)_2$ hybrid nanoflowers exhibited relatively high activity. Furthermore, the highest activity of the hNF-lipase was obtained when calcium phosphate was used as the inorganic component. Zhang et al found that Ca^{2+} could improve the activity of a lipase named ZC12 from *Psychrobacter sp*. ZY124 in hybrid nanoflowers [41]. They considered that Ca^{2+} induced self-assemble, but also activated the enzyme activity by inducing conformational changes in lipase $ZC1_2$. Furthermore, lipase ZC12 retained its "active form" after the immobilization [41, 42]. In order to confirm whether calcium ions induce conformational change of lipase in the lipase/$Ca_3(PO_4)_2$ hybrid nanoflowers, FTIR experiments were performed to analyze the lipase secondary structure variation. The results were shown in Table 2. Compared with free lipase, lipase/Ag_3PO_4 hybrid nanoflowers, lipase/$AlPO_4$ hybrid nanoflowers and lipase/$FePO_4$ hybrid nanoflowers, the lipase in the lipase/$Ca_3(PO_4)_2$ hybrid nanoflowers exhibited a decrease in α-helix and β-turn content. However, random coil content increased in the lipase in the

lipase/$Ca_3(PO_4)_2$ hybrid nanoflowers (Table 2). These results coincide with observations by Liu et al. who reported that the active site of free lipase was occluded by α-helix in the closed conformation (called lid), the conformational transition could lead to a decrease in α-helix and an increase in random coil [43]. The lipase with the "open" conformation was immobilized in calcium phosphate nanocrystals by interacted with the specific calcium binding pocket, which allows easier access to the substrate [42,43]. On the contrary, other metal ions (Ag^+, Al^{3+}, Fe^{3+}), could not induce the "open" conformation of the lipase. Therefore, the lipase/$Ca_3(PO_4)_2$ hybrid nanoflowers exhibited higher activity than other nanoflowers.

3.3 Influences of preparation conditions on the activity of the hNF-lipase

It is well known that the synthesis conditions have a great influence on the activity of the hNF-lipase. For example, Zhang et al. found that lipase content of the lipase hybrid nanoflower could be affected by adjusting lipase concentration, reaction temperature and stirring form [27]. Ke et al. reported that PBS concentration and lipase loading could affect immobilization efficiency of the lipase hybrid nanoflower [36]. To further understand the changes on activity of the formed hNF-lipase under the various reaction parameters, effects of various synthesis conditions including phosphate radical concentration in PBS, lipase concentration, Ca^{2+} concentration, and pH value activity of the hNF-lipase were systematically investigated. The results were shown in Fig. 6. Low activity of the hNF-lipase was observed in low phosphate radical concentration (<2 mM). With increasing phosphate radical concentration (>2 mM), the activity of hNF-lipase increased. The maximum activity was obtained when

phosphate radical concentration was 7 mM (Fig. 6a). Furthermore, it was found that with increase of lipase concentration the activity of the hNF-lipase increased significantly. However, a further increase of lipase concentration (>0.02 mg/mL) resulted in decrease of activity of the hNF-lipase (Fig. 6b). In addition, the activity of the hNF-lipase was closely related to Ca^{2+} concentration. The activity of the hNF-lipase was increased dramatically with the increase of Ca^{2+} concentration (Fig. 6c). Maximum activity of the hNF-lipase was obtained at 12.5 mM Ca^{2+} concentration. Besides, when pH value of PBS was higher than 7, activity of the hNF-lipase basically unchanged. However, low activity of the hNF-lipase was observed when the pH of PBS is 6 (Fig. 6d).

3.4 Effects of various surfactants on the activity of the hNF-lipase

It is generally known that the catalytic activity of lipase can be dramatically increased by the surfactant activation (interfacial activation) [30].With an aim to further improve the catalytic activity of the hNF-lipase, the lipase activated by surfactants were sequentially used for the hNF-lipase preparation. Four surfactants (including CTAB, DTAB, TX-100, and Tween 80) were used to activate lipase, and the results are shown in Fig. 7. Compared with hNF-lipase, the activated hNF-lipase with tween-80 showed a substantial hyperactivation, and the maximum relative activity of the activated hNF-lipase reached 172% when 0.15 mM Tween-80 was used as activator. However, both CTAB and DTAB showed little effect on the activity of hNF-lipase. Interestingly, the activity of hNF-lipase was decreased when TX-100 was added, indicating negative effect of TX-100 on the activity of lipase. Therefore,

Tween 80 at a concentration of 0.15 mM was the optimal activator to for the preparation of the hNF-lipase. The previous reports showed that surfactants could induce lipase changes from closed conformation to open conformation [44, 45]. All of these results demonstrated that the surfactants play an important role in the activation of lipase.

3.5 Catalytic activity of lipase nanoflowers

The results of kinetic parameters (K_m and V_{max}) are listed in Table 3. K_m value of the lipase nanoflowers was higher than the free lipase, indicating the high diffusion resistance between substrate and lipase. However, higher V_{max} indicated the high catalytic efficiency of hNF-lipase relative to the free lipase. It was worth noting that the activated hNF-lipase displayed higher V_{max}/K_m than the free lipase and the hNF-lipase, respectively. The results further demonstrated that the activated hNF-lipase have the highest catalytic efficiency among all of lipase samples. This increased catalytic efficiency is due to the active conformation of lipase in the activated hNF-lipase. In addition, effects of temperature and pH on the activity of lipase samples were determined (Fig. 8). The optimum temperature for the hybrid nanoflowers was 40 °C, which was in consonance with free lipase (Fig 8a). Furthermore, it was found that the optimum pH for free lipase, hNF-lipase and activated hNF-lipase was at pH 4 (Fig 8b).

3.6 Stability of the hNF-lipase

The stability of the immobilized enzymes is important for industrial applications. Therefore, the stabilities of lipase samples were tested against heat and various

denaturants (Fig. 9). Results showed that the lipase nanoflowers presented excellent thermal stability at 70 °C for 30 min. The hNF-lipase and activated hNF-lipase retained 56% and 85% of their initial activities, respectively. However, free lipase maintained only 49% of its initial activity (Fig. 9a). In addition, the hybrid nanoflowers also showed higher stability against denaturants including 6 M urea, 2% (W/V) SDS, and 95% ethanol than that to the free counterpart (Fig. 9b). For example, after incubation in 6 M urea for 30 min, the hNF-lipase and activated hNF-lipase retained 92.42% and 93.24% of their residual activities, respectively. However, the free lipase maintained only 51.39% of its initial activity. Besides, the storage stability of lipase samples was determined at 25 °C for 27 days. The results showed that the hNF-lipase and activated hNF-lipase still retained 90% and 80% of their initial activities respectively. However, the free lipase only maintained 58% of its initial activity. In addition, the reusability of the lipase nanoflowers was investigated (Fig. 9d). It can be found that the hNF-lipase and activated hNF-lipase were capable of preserving 61% and 68% of their original activities after six consecutive cycles. Overall, the findings indicated the potential of hNF-lipase for diverse industrial applications.

4. Conclusions

In conclusion, we systematically investigated the influences of metal ions with different valence, surfactants, and synthesis conditions on the shape and activity of the lipase hybrid nanoflowers. The synthesized lipase hybrid nanoflowers using bivalence metal ions (Ca^{2+}, Mn^{2+}, and Zn^{2+}) presented more higher activity than that of using univalent metal ions (Ag^{+}) or trivalent metal ions (Al^{3+} or Fe^{3+}). Especially, the

lipase/$Ca_3(PO_4)_2$ hybrid nanoflowers displayed 9, 12, and 61 folds higher activity than lipase/Ag_3PO_4 hybrid nanoflowers, lipase/$AlPO_4$ hybrid nanoflowers, and lipase/$FePO_4$ nanoflowers, respectively. Ca^{2+} not only induced self-assemble of nanoflowers, but also activated the lipase from *A. oryzae*. The activity of the hNF-lipase was further increased by the surfactant activation. The activated hNF-lipase displayed an 172% increase in activity using 0.15 mM Tween-80 as an activity inducer. At the same time, the hNF-lipase and activated hNF-lipase exhibited high stability against heat and various denaturants. Furthermore, the hybrid nanoflowers demonstrated excellent reusability. In conclusion, lipase nanoflowers would be an efficient immobilized lipase with broad-spectrum potential for practical applications.

CRediT author statement

J.Cui. and S.Jia. designed the experimental scheme and analyzed the experimental data. C.Li. Z.Zhang, and J.Zhao. did the most of the sample preparation and characterizations. Y.Jiang. M.Bilal, and Y. Hong wrote and revised the manuscript.

Declaration of interests

The authors declare that they have no known competing financial interests or personal relationships that could have appeared to influence the work reported in this paper.

Acknowledgements

This work is partially supported by the National Natural Science Foundation of China (project no. 21676069). Dr. J. D. Cui also thanks supports from the Key Projects of

Tianjin Natural Science Foundation, China (project no. 19JCZDJC38100), and Undergraduate Laboratory Funds for Innovation of TUST (1931A201).

Reference

[1] F. Hasan, A.A. Shah, A. Hameed, Industrial applications of microbial lipases, Enzyme. Microb. Tech. 39 (2006) 235-251.

[2] M. Bilal, M. Asgher, H.M.N. Iqbal, H.B. Hu, X.C. Zhang, Delignification and fruit juice clarification properties of alginate-chitosan-immobilized ligninolytic cocktail, Lwt-Food Sci Technol. 80 (2017) 348-354.

[3] W. Li, H. Wu, B.G. Liu, X.D. Hou, D.J. Wan, W.Y. Lou, J. Zhao, Highly efficient and regioselective synthesis of dihydromyricetin esters by immobilized lipase, J Biotechnol. 199 (2015) 31-37.

[4] S. Sanchez, A.L. Demain, Enzymes and bioconversions of industrial, pharmaceutical, and biotechnological significance, Org Process Res Dev. 15 (2011) 224-230.

[5] M. Bilal, M. Asgher, R. Parra-Saldivar, H. Hu, W. Wang, X. Zhang, H.M.N. Iqbal, Immobilized ligninolytic enzymes: An innovative and environmental responsive

technology to tackle dye-based industrial pollutants-A review, Sci. Total Environ. 576 (2017) 646-659.

[6] M. Ashraf, N.A. Akram, Improving salinity tolerance of plants through conventional breeding and genetic engineering: An analytical comparison, Biotechnol Adv. 27 (2009) 744-752.

[7] H.T. Hwang, Q. Feng, C. Yuan, X. Zhao, A. Varma, Review: Lipase-catalyzed process for biodiesel production: Protein engineering and lipase production, Biotechnol.Bioeng. 111 (2014) 639-653.

[8] E.M. Nordwald, J.L. Kaar, Stabilization of enzymes in ionic liquids via modification of enzyme charge, Biotechnol. Bioeng. 110 (2013) 2352-2360.

[9] G. DeSantis, J.B. Jones, Chemical modification of enzymes for enhanced functionality, Curr Opin Biotech. 10 (1999) 324-330.

[10] K. Matsumoto, B.G. Davis, J.B. Jones, Chemically modified "polar patch" mutants of subtilisin in peptide synthesis with remarkably broad substrate acceptance: Designing combinatorial biocatalysts, Chem-Eur J. 8 (2002) 4129-4137.

[11] S.W. Ding, A.A. Cargill, I.L. Medintz, J.C. Claussen, Increasing the activity of immobilized enzymes with nanoparticle conjugation, Curr Opin Biotech. 34 (2015) 242-250.

[12] J. Ge, D.N. Lu, Z.X. Liu, Z. Liu, Recent advances in nanostructured biocatalysts, Biochem Eng J. 44 (2009) 53-59.

[13] H.R. Lee, M. Chung, M.I. Kim, S.H. Ha, Preparation of glutaraldehyde-treated lipase-inorganic hybrid nanoflowers and their catalytic performance as immobilized

enzymes, Enzyme. Microb. Tech. 105 (2017) 24-29.

[14] Y.T. Zhang, T.T. Zhi, L. Zhang, H. Huang, H.L. Chen, Immobilization of carbonic anhydrase by embedding and covalent coupling into nanocomposite hydrogel containing hydrotalcite, Polymer. 50 (2009) 5693-5700.

[15] F.M. Veronese, Peptide and protein PEGylation: a review of problems and solutions, Biomaterials. 22 (2001) 405-417.

[16] J.D. Cui, S.Z. Ren, T. Lin, Y.X. Feng, S.R. Jia, Shielding effects of Fe^{3+}-tannic acid nanocoatings for immobilized enzyme on magnetic Fe_3O_4@silica core shell nanosphere, Chem. Eng. J. 343 (2018) 629-637.

[17] M. Romero-Arcos, J.F. Perez-Robles, M.G. Garnica-Romo, M.S. Luna-Martinez, M.A. Gonzalez-Reyna, Synthesis and functionalization of carbon nanotubes and nanospheres as a support for the immobilization of an enzyme extract from the mushroom *Trametes versicolor*, J. Mater. Sci. 54 (2019) 11671-11681.

[18] M.F. Wang, W. Qi, R.X. Su, Z.M. He, Advances in carrier-bound and carrier-free immobilized nanobiocatalysts, Chem. Eng. Sci. 135 (2015) 21-32.

[19] Z. Zhou, M. Hartmann, Progress in enzyme immobilization in ordered mesoporous materials and related applications, Chem. Soc. Rev. 42 (2013) 3894-3912.

[20] J.J. Sun, R. Yendluri, K. Liu, Y. Guo, Y.R. Lvov, X.H. Yan, Enzyme-immobilized clay nanotube-chitosan membranes with sustainable biocatalytic activities, Phys. Chem. Chem. Phys. 19 (2017) 562-567.

[21] X.H. Xu, X. Qi, X.Q. Wang, X.Y. Wang, Q. Wang, H. Yang, Y.C. Fu, S.Z. Yao,

Highly efficient enzyme immobilization by nanocomposites of metal organic coordination polymers and carbon nanotubes for electrochemical biosensing, Electrochem. Commun. 79 (2017) 18-22.

[22] X.H. Liu, Y.C. Fang, X. Yang, Y. Li, C. Wang, Electrospun epoxy-based nanofibrous membrane containing biocompatible feather polypeptide for highly stable and active covalent immobilization of lipase, Colloid Surface B. 166 (2018) 277-285.

[23] J.D. Cui, T. Lin, Y.X. Feng, Z.L. Tan, S.R. Jia, Preparation of spherical cross-linked lipase aggregates with improved activity, stability and reusability characteristic in water-in-ionic liquid microemulsion, J. Chem. Technol. Biotechnol. 92 (2017) 1785-1793.

[24] J. Ge, J. Lei, R.N. Zare, Protein–inorganic hybrid nanoflowers, Nat. Nanotechnol. 7 (2012) 428-432.

[25] Z. Lin, Y. Xiao, L. Wang, Y. Yin, J. Zheng, H. Yang, G. Chen, Facile synthesis of enzyme-inorganic hybrid nanoflowers and their application as an immobilized trypsin reactor for highly efficient protein digestion. RSC.Adv. 4 (2014) 13888-13891.

[26] Y. Yin, Y. Xiao, G. Lin, Q. Xiao, Z. Lin, Z. Cai, An enzyme-inorganic hybrid nanoflower based immobilized enzyme reactor with enhanced enzymatic activity, J. Mater. Chem. B. 3 (2015) 2295-2300.

[27] B. Zhang, P. Li, H. Zhang, H. Wang, X. Li, L. Tian, N. Ali, Z. Ali, Q. Zhang, Preparation of lipase/$Zn_3(PO_4)_2$ hybrid nanoflower and its catalytic performance as an immobilized enzyme, Chem. Eng. J. 291 (2016) 287-297.

[28] J. Cui, Y. Zhao, R. Liu, C. Zhong, S. Jia, Surfactant-activated lipase hybrid

nanoflowers with enhanced enzymatic performance, Sci Rep-Uk. 6 (2016) 27928-27940.

[29] Z. X. Lei, C. L. Gao, L. Chen, Y. T. He, W. D. Ma, Z. Lin, Recent advances in biomolecule immobilization based on self-assembly: organic–inorganic hybrid nanoflowers and metal–organic frameworks as novel substrates. J. Mater. Chem. B. 6(2018) 1581-1594.

[30] J .D.Cui, S. R.Jia. Organic-inorganic hybrid nanoflowers: A novel host platform for immobilizing biomolecules. Coordin Chem Rev. 352(2017) 249-263.

[31] J. Yamoneka, P. Malumba, G. Lognay, F. Bera, C. Blecker, S. Danthine, Enzymatic inter-esterification of binary blends containing *Irvingia gabonensis* seed fat to produce Cocoa butter substitute, Eur. J. Lip. Sci. Tech. 120 (2018).

[32] S. Shah, S. Sharma, M.N. Gupta, Biodiesel preparation by lipase-catalyzed transesterification of Jatropha oil, Energy & Fuels. 18 (2004) 154-159.

[33] E.C.G. Aguieiras, D.S.N. de Barros, R. Fernandez-Lafuente, D.M.G. Freire, Production of lipases in cottonseed meal and application of the fermented solid as biocatalyst in esterification and transesterification reactions, Renew. Energ. 130 (2019) 574-581.

[34] N.B. Melani, E.B. Tambourgi, E. Silveira, Lipases: From Production to Applications, Sep. Purif. Rev. (2019) 1-16.

[35] J.C.J. Quilles, R.R. Brito, J.P. Borges, C.C. Aragon, G. Fernandez-Lorented, D.A. Bocchini-Martins, E. Gomes, R. Da Silva, M. Boscolo, J.M. Guisan, Modulation of the activity and selectivity of the immobilized lipases by surfactants and solvents,

Biochem Eng J. 93 (2015) 274-280.

[36] C. Ke, Y. Fan, Y. Chen, L. Xu, Y. Yan, A new lipase–inorganic hybrid nanoflower with enhanced enzyme activity, RSC. Adv. 6 (2016) 19413-19416.

[37] J. Gao, W. Kong, L. Zhou, Y. He, L. Ma, Y. Wang, L. Yin, Y. Jiang, Monodisperse core-shell magnetic organosilica nanoflowers with radial wrinkle for lipase immobilization, Chem. Eng. J. 309 (2017) 70-79.

[38] C. Yang, F. Wang, D. Lan, C. Whiteley, B. Yang, Y. Wang, Effects of organic solvents on activity and conformation of recombinant *Candida antarctica* lipase A produced by *Pichia pastoris*, Process. Biochem. 47 (2012) 533-537.

[39] S. Escobar, S. Velasco-Lozano, C.-H. Lu, Y.-F. Lin, M. Mesa, C. Bernal, F. López-Gallego, Understanding the functional properties of bio-inorganic nanoflowers as biocatalysts by deciphering the metal-binding sites of enzymes, J. Mater. Chem. B. 5 (2017) 4478-4486.

[40] W. Jiang, X. Wang, J. Yang, H. Han, Q. Li, J. Tang, Lipase-inorganic hybrid nanoflower constructed through biomimetic mineralization: A new support for biodiesel synthesis, J Colloid Interface Sci. 514 (2018) 102-107.

[41] Y. Zhang, F. Ji, J. Wang, Z. Pu, Y. Bao, Purification and characterization of a novel organic solvent-tolerant and cold-adapted lipase from *Psychrobacter sp.* ZY124, Extremophiles. 22 (2018) 1-14.

[42] Y. Zhang, W. Sun, N.M. Elfeky, Y. Wang, D. Zhao, H. Zhou, J. Wang, Y. Bao, Self-assembly of lipase hybrid nanoflowers with bifunctional Ca^{2+} for improved activity and stability, Enzyme Microb. Technol. 132 (2020) 109408.

[43] Y. Liu, D. Chen, Y. Yan, C. Peng, L. Xu, Biodiesel synthesis and conformation of lipase from *Burkholderia cepacia* in room temperature ionic liquids and organic solvents, Bioresource Technol. 102 (2011) 10414-10418.

[44] Yang, Zhang, Surfactant imprinting hyperactivated immobilized lipase as efficient biocatalyst for biodiesel production from waste cooking oil, Catalysts. 9 (2019) 914.

[45] F. Kartal, Enhanced esterification activity through interfacial activation and cross-linked immobilization mechanism of *Rhizopus oryzae* lipase in a nonaqueous medium, Biotechnol. Progr. 32 (2016) 899-904.

Table 1. The relative activity of hNF-lipase synthesized using metal ions with a range of different valence.

Biocatalysts	Relative activity (%)
hNF-lipase/Ag_3PO_4	4.87±0.008
hNF-lipase/$Mn_3(PO_4)_2$	24.11±0.12
hNF-lipase/$Zn_3(PO_4)_2$	30.20±0.15
hNF-lipase/$Ca_3(PO_4)_2$	43.05±0.18
hNF-lipase/$AlPO_4$	3.48±0.07
hNF-lipase/$FePO_4$	0.71±0.008
hNF-lipase/$Mg_3(PO_4)_2$	0 (No precipitation)

Table 2. Quantitative estimation of the secondary structure elements of free lipase, and lipase hybrid nanoflowes using different metal ions

biocatalysts	α-Helix (%)	β-Sheet (%)	β-Turn (%)	Random coil (%)
Free lipase	23.39±0.12	43.74±0.09	19.35±0.13	8.46±0.09
hNF-lipase/Ag_3PO_4	18.13±0.11	38.32±0.08	16.55±0.09	6.96±0.08
hNF-lipase/$Ca_3(PO_4)_2$	17.98±0.12	29.00±0.11	12.69±0.12	15.08±0.11
hNF-lipase/$AlPO_4$	21.08±0.13	46.29±0.13	19.55±0.11	7.07±0.07
hNF-lipase/$FePO_4$	21.08±0.12	34.70±0.08	15.21±0.09	2.29±0.02

Table 3. The kinetic parameters of free lipase, lipase/$Ca_3(PO_4)_2$ hybrid nanoflowers and activated lipase/$Ca_3(PO_4)_2$ hybrid nanoflowers

Biocatalysts	K_m **(mM)**	V_{max} **(mM/min)**	V_{max}/K_m
Free lipase	1.606±0.008	0.122±0.006	0.076±0.003
hNF-lipase/$Ca_3(PO_4)_2$	11.908±0.06	0.853±0.004	0.072±0.003
Activated hNF-lipase/$Ca_3(PO_4)_2$	5.96±0.03	0.458±0.002	0.077±0.003

Figure legends

Figure 1 Schematic illustration of the preparation of hNF-lipase/$Ca_3(PO_4)_2$ and activated hNF-lipase/$Ca_3(PO_4)_2$.

Figure 2 SEM, TEM and CLSM images of hNF-lipase/$Ca_3(PO_4)_2$.

Figure 3 EDS patterns of (a) hNF-lipase and (b) $Ca_3(PO_4)_2$.

Figure 4 FTIR spectra (a) of free lipase, $Ca_3(PO_4)_2$, hNF-lipase and activated hNF-lipase and (b) XRD patters of $Ca_3(PO_4)_2$, hNF-lipase and activated hNF-lipase.

Figure 5 SEM images of hNF-lipase synthesized using metal ions with different valence (a-e). (a) Ag^+; (b) Ca^{2+}; (c) Mn^{2+} ; (d) Zn^{2+}; (e) Al^{3+}; (f) Fe^{3+}.

Figure 6 Optimization of synthesis conditions of hNF-lipase. (a) phosphate radical concentration, (b) lipase concentration, (c) calcium chloride concentration, and (d) pH of PBS.

Figure 7 Effect of different surfactants on the activity of hNF-lipase.

Figure 8 Effect of (a) temperature and (b) pH on the activity of free lipase, hNF-lipase, and activated hNF-lipase.

Figure 9 Stability of free lipase, hNF-lipase, and activated hNF-lipase against (a) temperature; (b) denaturants; (c) storage stability of free lipase, hNF-lipase, and activated hNF-lipase; (d) reusability of hNF-lipase and activated hNF-lipase.

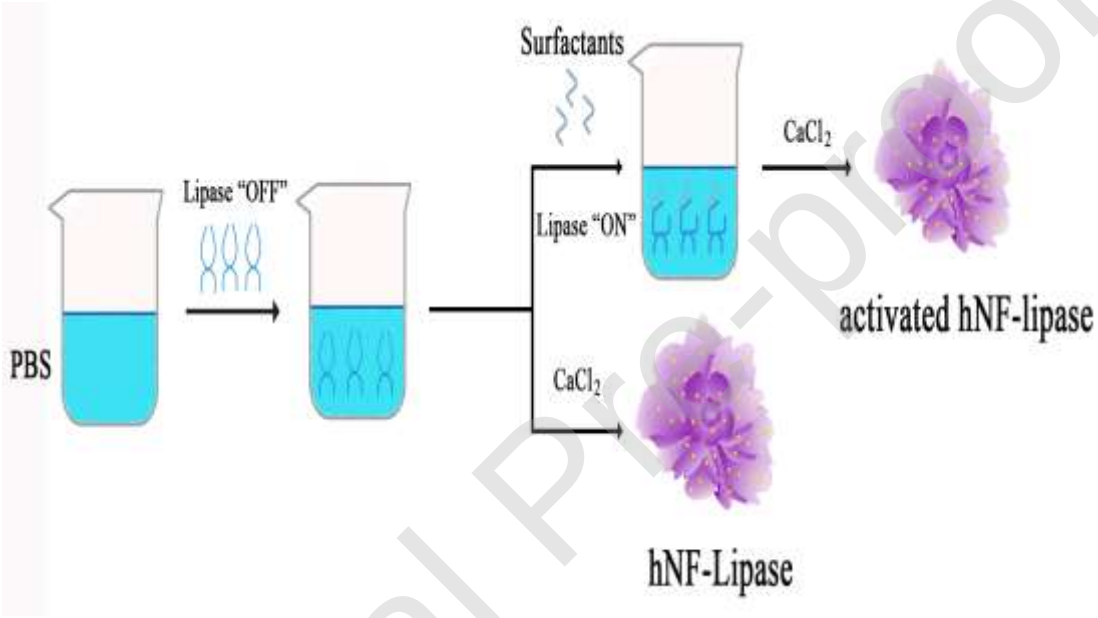

Figure 1

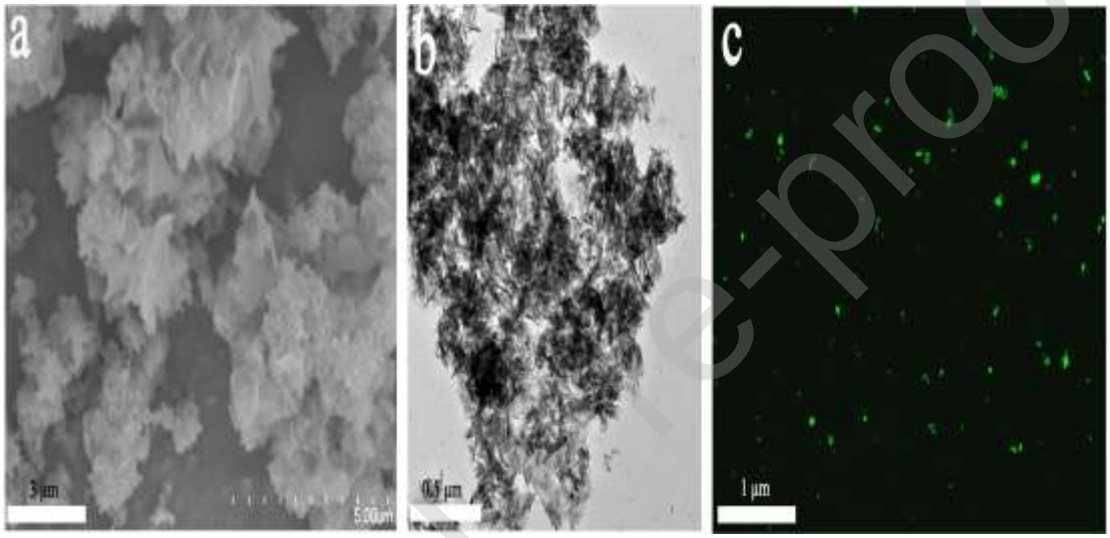

Figure 2

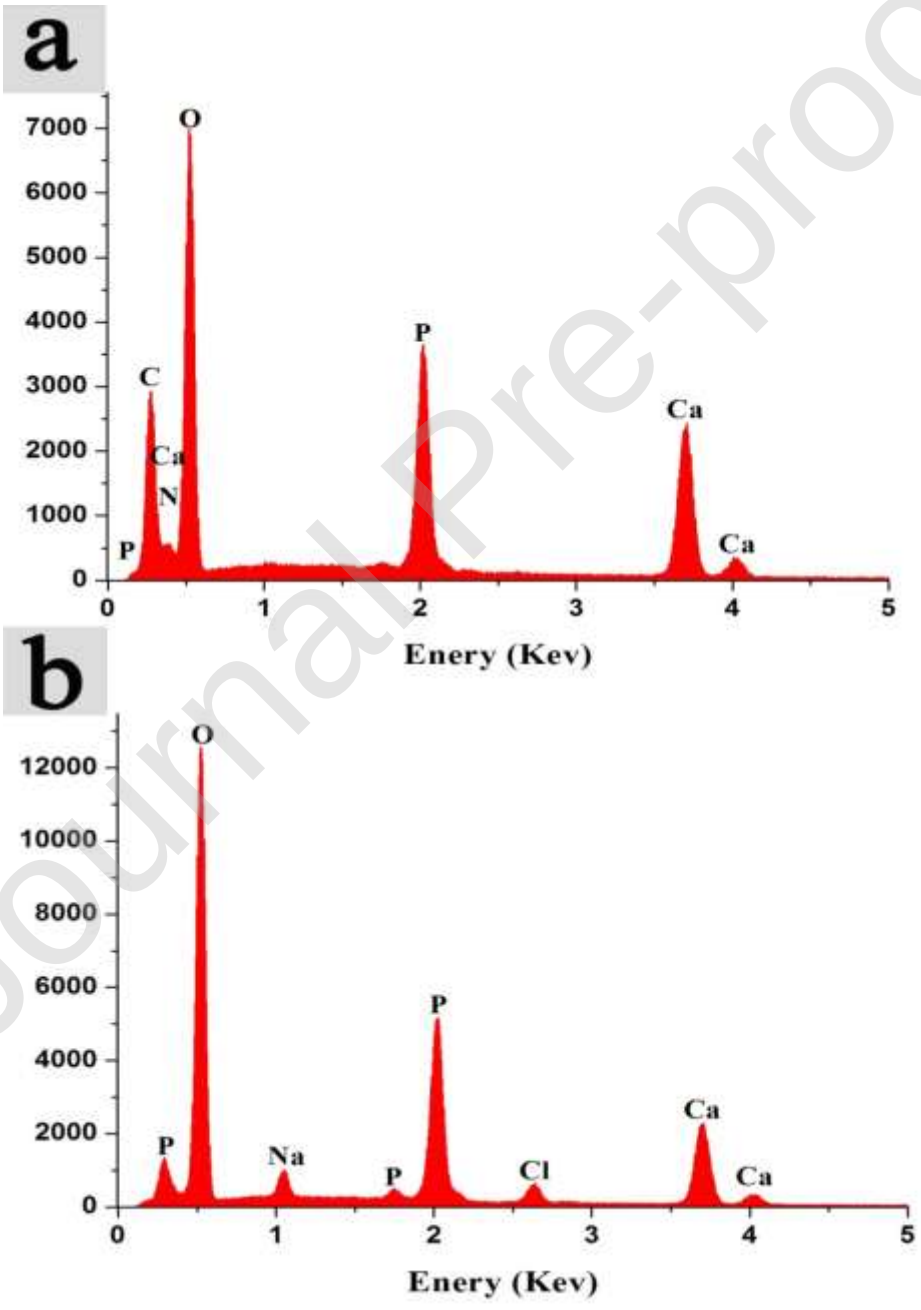

Figure 3

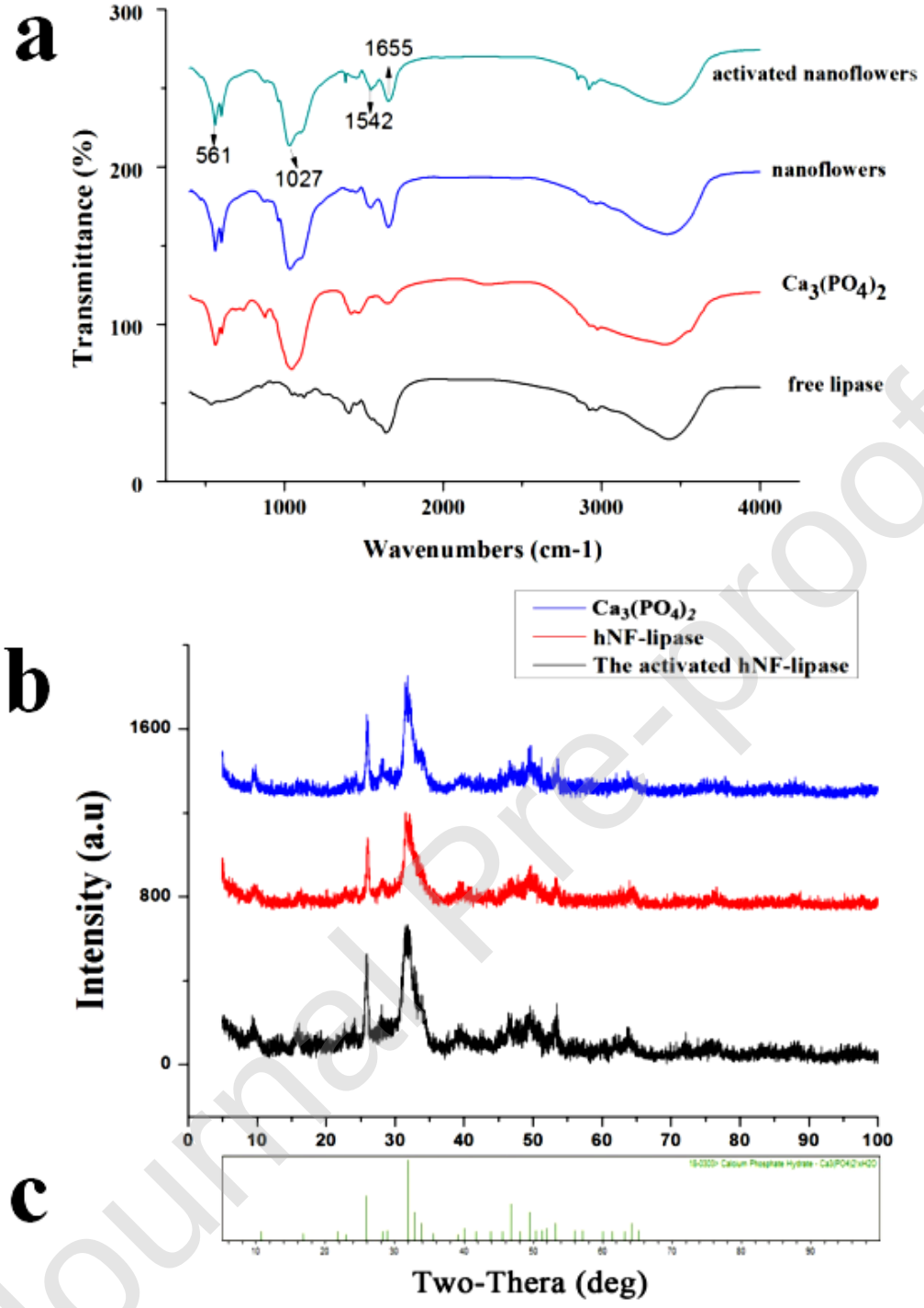

Figure 4

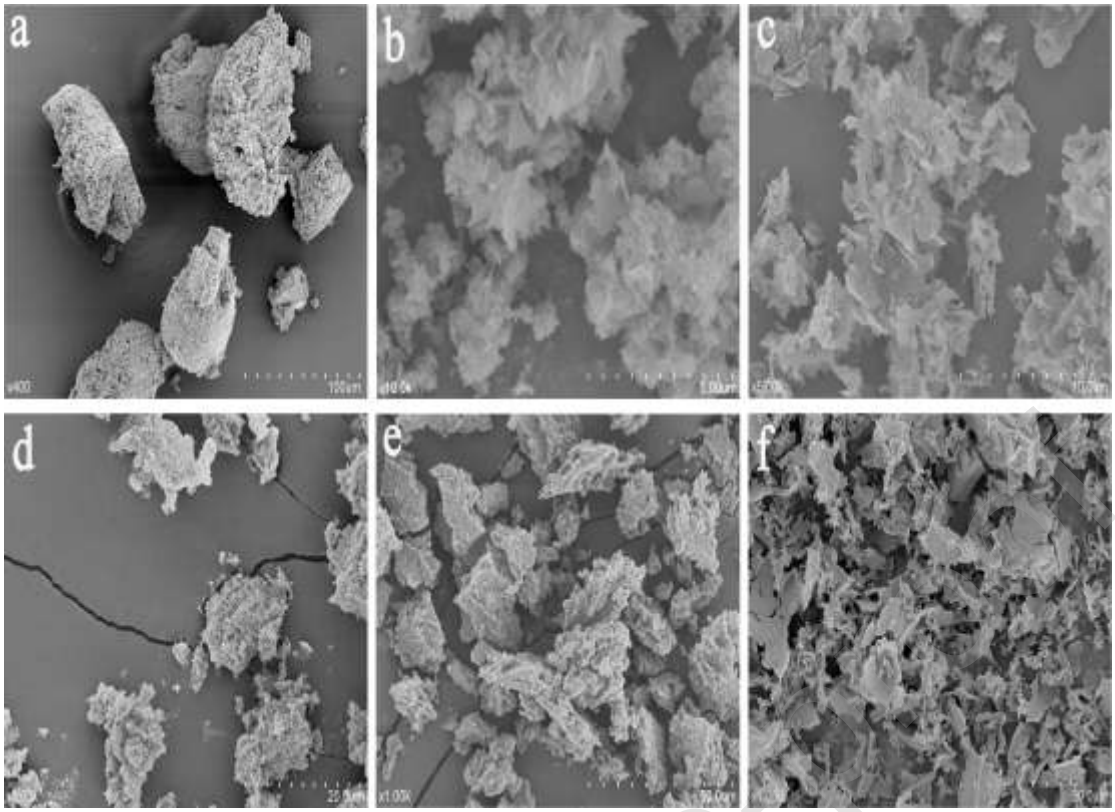

Figure 5

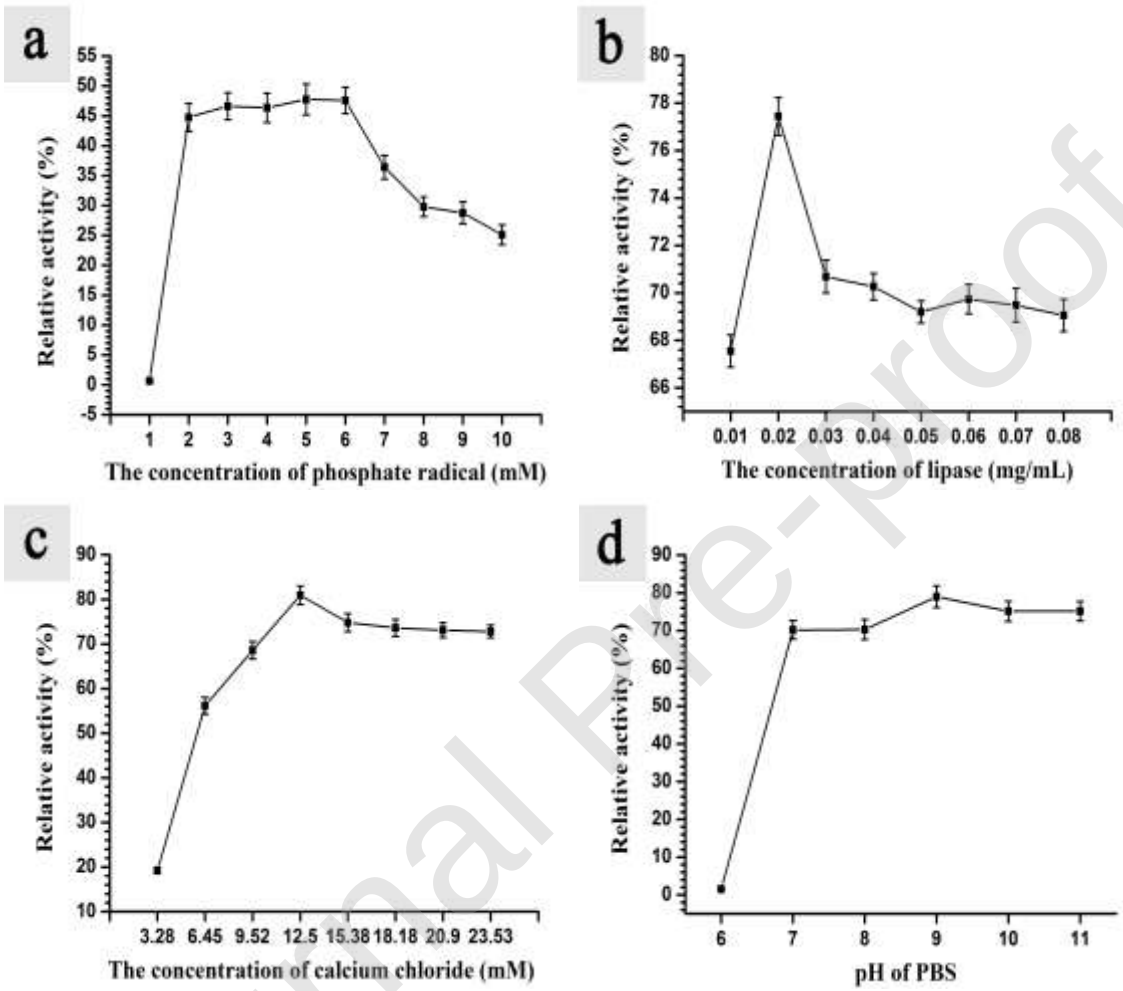

Figure 6

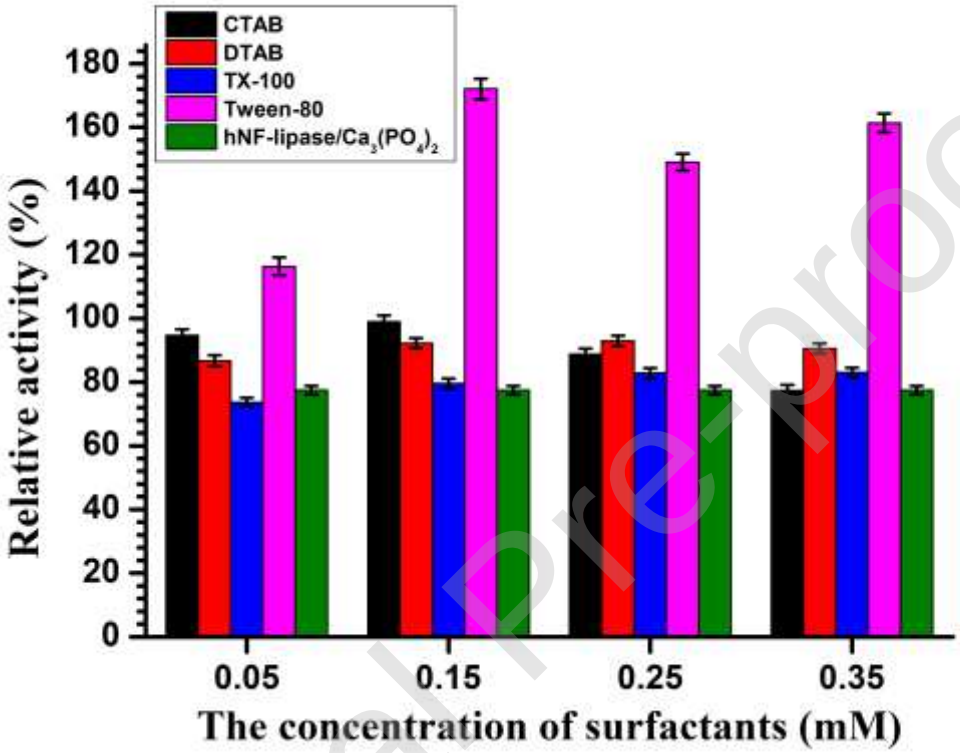

Figure 7

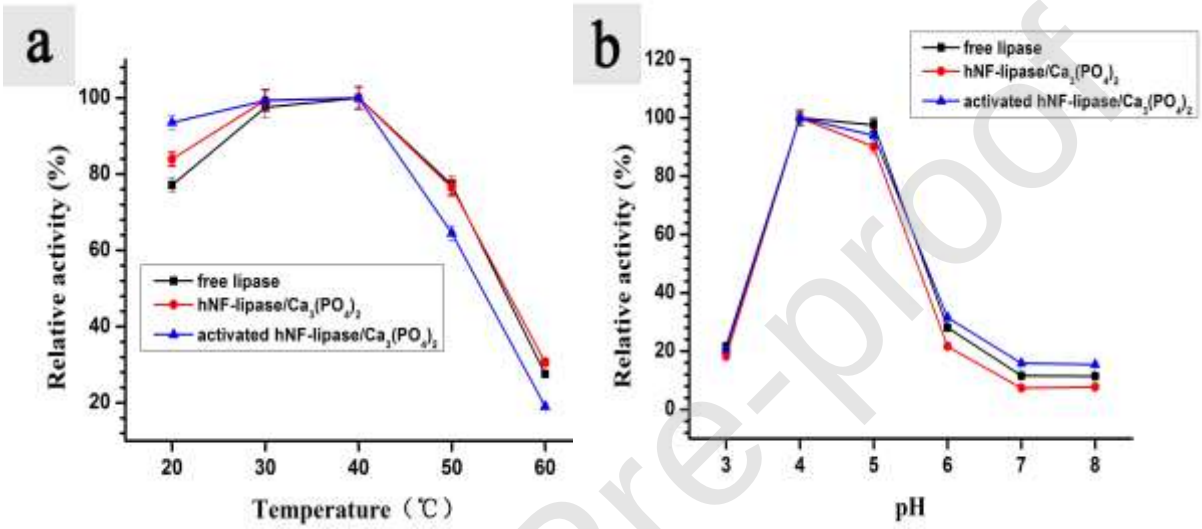

Figure 8

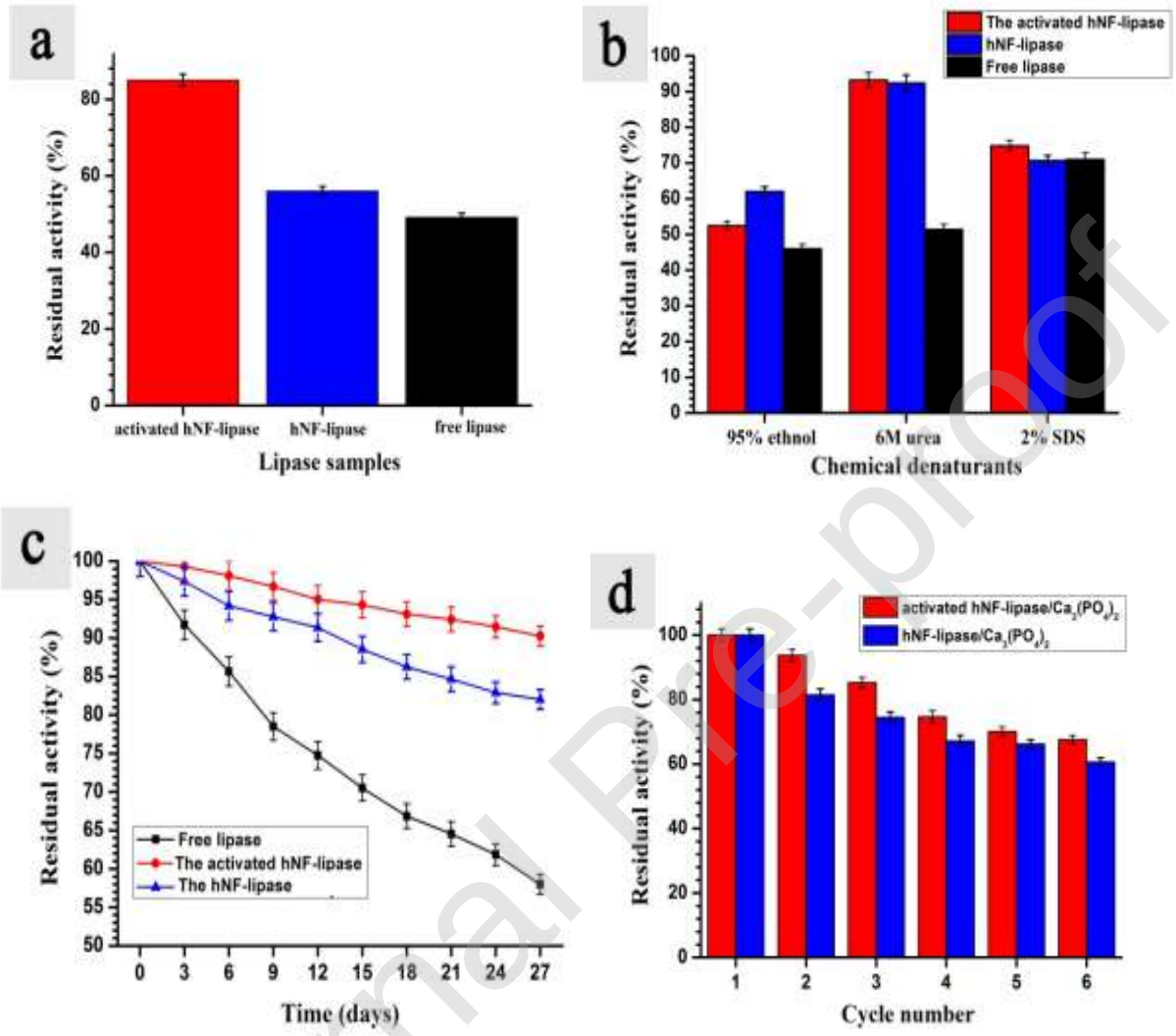

Figure 9